Rapid numerical assessment of process-induced dimensional changes and residual stresses in large aerospace composite parts

Proceedings of the ASME 2024
Aerospace Structures, Structural Dynamics, and Materials Conference
SSDM2024
April 29 - May 1, 2024, Renton, Washington

SSDM2024-121518

RAPID NUMERICAL ASSESSMENT OF PROCESS-INDUCED DIMENSIONAL CHANGES AND RESIDUAL STRESSES IN LARGE AEROSPACE COMPOSITE PARTS

Enrico Zappino[1]
Politecnico di Torino
enrico.zappino@polito.it

Navid Zobeiry[2]
University of Washington
navidz@uw.edu

Rebecca Masia[1]
Politecnico di Torino
rebecca.masia@polito.it

Marco Petrolo[1]
Politecnico di Torino
marco.petrolo@polito.it

[1]MUL2 Lab, Department of Mechanical and Aerospace Engineering, Politecnico di Torino, Turin, Italy
[2]Department of Materials Science and Engineering, University of Washington, Seattle, WA, 98195, USA

ABSTRACT

Process-induced deformations (PIDs) are a major issue in fabricating composite aerostructures, hindering the assembly process. For example, geometrical mismatches between spars and wing skins can lead to considerable assembly delays during the assembly of a composite wing box. In these cases, shims with specific geometries, based on the mismatch of the original parts, are fabricated and used to meet the current tight tolerances in aerospace. Given such parts 'complex and large geometry, process simulations to assess PIDs are often quite slow. This paper aims to evaluate the effect of geometry and design details on PIDs and residual stresses of composite spars efficiently and robustly. Typical cross-sectional geometries such as the Omega shape are considered. Furthermore, the impact of design details, including ply drop-off, on PIDs such as spring-in angles, warpage, and 3D stress distributions are evaluated along long spars.

The structural modeling is handled using 1D higher-order layer-wise theories based on the Carrera Unified Formulation (CUF) to speed up the process simulation of large parts. Such theories are necessary to detect relevant mechanical behaviors: transverse stretching, shear deformation, anisotropy, and layer-wise changes of the physical properties. On the other hand, using 1D theories significantly impacts the computational overhead as there are no aspect ratio constraints on the finite elements (FE), thus leading to much fewer degrees of freedom than 2D or 3D models. Although 1D, the model provides the complete 3D strain and stress fields as the primary unknowns – in this paper, pure displacements – are expanded using higher-order Lagrange polynomials to remove the typical assumptions of 1D modes, e.g., rigid cross-sections, null or constant shear distributions.

The evolution of material properties, such as the evolution of the degree of cure, viscoelastic moduli, and free strains, are characterized using established DSC and DMA tests. Accordingly, a cure-hardening instantaneously linear elastic (CHILE) constitutive model is adopted for numerical simulations. The results are verified through analytical formulations and published data in the literature. The proposed simulation approach allows for rapid evaluation of residual stresses and PIDs. Due to its numerical efficiency, the effect of various design parameters can be quickly evaluated. Therefore, this tool can explore the design space for large and complex composite parts and potentially develop mitigation strategies.

1. INTRODUCTION

Composite materials are standard solutions in numerous high-performance structural applications, notably aerospace. The exceptional combination of high stiffness and strength, alongside their lightweight nature, make carbon fiber-reinforced polymers the preferred choice in many engineering applications. A significant challenge in the design of polymer-based components lies in the alteration of shape and dimensions during manufacturing. This aspect is especially critical for the final structural integrity and performance of the components, as well as the assembly process of composite structures. The complexity of the component's shape further amplifies this challenge, a factor increasingly relevant given the advanced and diverse applications of composite materials in recent times.

In the curing stage of thermoset composites, components undergo high temperature and pressure cycles, potentially leading to process-induced flaws. These issues stem from the material's anisotropic behavior and are closely linked to residual

stresses and localized deformations. These residual stresses cause deformation upon demolding, which, upon assembly, can significantly reduce the safety margin and increase the risk of early failure in the component's operational life [1,2]. Therefore, the precise forecasting and management of these residual defects are crucial in the manufacturing process of such components.

Over the last years, significant research efforts have been directed towards predicting and reducing process-induced stresses and deformations caused during manufacturing. Employing numerical simulations has emerged as a key strategy to reduce time and resources while enhancing the precision of these predictions. Especially noteworthy is the escalating complexity of the analyzed components, such as ply drop-off models [3] and L-C-Z-shape models [4,5,6], demand increasingly sophisticated simulation techniques.

Recent research has explored these models through both analytical and numerical approaches. A key challenge in addressing process-induced deformation is accurately modeling the thickness direction, where traditional numerical models often fall short. Consequently, three-dimensional modeling is crucial for simulations that account for process-induced changes.

This study focuses on predicting process-induced deformations and stresses in various configurations, including the ply drop-off and Omega-shape geometries, with distinct stacking sequences. The outcomes of the numerical analysis are thoroughly analyzed to understand the predicted behaviors. Employing the Carrera Unified Formulation [7], the study models complex three-dimensional structures into more manageable one-dimensional models without compromising accuracy, achieving a fidelity comparable to full three-dimensional models.

2. HIGHER-ORDER NUMERICAL MODEL

The numerical approach employs the well-established Carrera Unified Formulation (CUF) to develop a higher-order beam theory [7]. According to CUF, the complete three-dimensional displacement field can be described in a compact manner:

$$\boldsymbol{u}(x,y,z) = \mathrm{F}_\tau(x,z) N_i(y) \boldsymbol{u}_{\tau i} \qquad (1)$$

where τ represents the number of expansion terms, and i denotes the number of the terms of the one-dimensional shape functions. The expansion functions, F_τ, utilized in this study are based on Lagrange polynomials, allowing a layer-wise description of the model. Every lamina can be described with a different kinematics model, achieving the desired level of accuracy. Quadratic nine-node Lagrange elements, defined as L9, are involved in the cross-section of the model, and cubic four-node elements B4 are utilized for the 1D FE discretization. Once the displacement field is derived from Eq. (1), the stress field can be evaluated using Hooke's law. The governing equations of the problem are derived using the Principle of Virtual Displacements (PVD), and the problem is solved by assembling the Fundamental Nuclei (FN) over the four characteristic indices of the CUF approach. The internal work of the problem can be expressed as:

$$\delta L_{int} = \int_V \delta \boldsymbol{\varepsilon}^T \boldsymbol{\sigma}\, dV = \delta \boldsymbol{u}_{sj}^T \int_V N_j F_s \boldsymbol{D}^T \boldsymbol{C}\, \boldsymbol{D}\, F_\tau N_i dV\ \boldsymbol{u}_{\tau i} = \delta \boldsymbol{u}_{sj}^T k^{ij\tau s} \boldsymbol{u}_{\tau i} \qquad (2)$$

where $k^{ij\tau s}$ is the FN of the problem., similarly the external work can be expressed in terms of CUF, and the FN of the external work, denoted as $\boldsymbol{f}^{js}$, can be computed.

2.1 Curing cycle numerical simulation

The numerical simulation of the curing cycle is based on the Cure-Hardening Instantaneously Linear Elastic (CHILE) constitutive model, which assumes that the material exhibits an instantaneous linear elastic response [8]. The curing simulation begins at the gelation point and follows an iterative process. In each analysis step, the elastic, thermal, and chemical properties of the composite component are updated. The external conditions of the autoclave are simulated throughout the entire process, and at each step, the increments of displacements are recorded. The solution at the end of the process is the cumulative summation of the incremental elastic solutions corresponding to each i-th step:

$$u = \sum_{i=1}^{N} \Delta u_i \qquad (3)$$

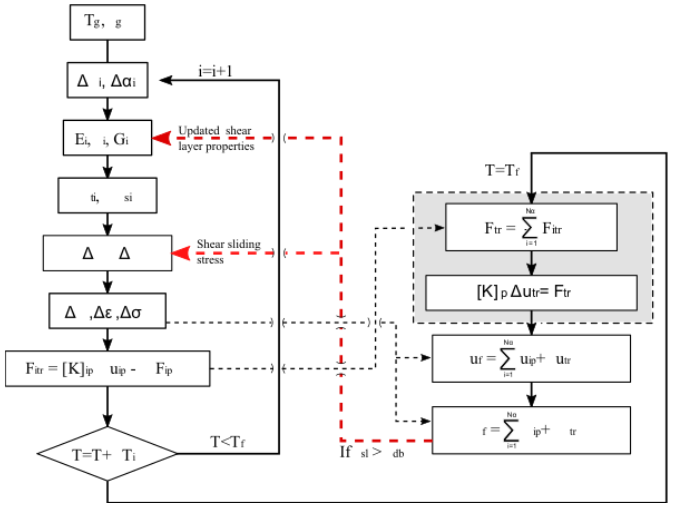

FIGURE 1: FLOWCHART OF THE CURING CYCLE NUMERICAL SIMULATION.

Similarly, the strain and stress fields developed during the process can be evaluated. To simulate the component's demolding from the tool, the force accumulated between the part and the tool is stored and applied to the part. The numerical simulation for the curing cycle process is illustrated in Fig. 1.

The curing cycle involved in the simulation features a heating step at 1 °C/min, followed by a hold temperature step at

180 °C for 120 minutes, and a final cool-down step. This leads to a total cycle time of approximately 333 minutes.

3. MATERIAL AND GEOMETRY

In this study, the selected composite material is Hexcel's AS4/8552 unidirectional prepreg. This prepreg's cured ply has an approximate thickness of 0.19 mm and consists of about 35% 8552 epoxy resin system by weight [9] and 65% AS4 HexTow carbon fibers with an Aerial weight of 190gsm [10] by weight. The tool and the shear layer in this study are composed of Invar, characterized by isotropic mechanical properties $\alpha = 1.56 \times 10{-}6$ /◦C.

The study involves two geometries. The first is a drop-off layer model, shown in Fig. 2, and the second is an Omega-shape model consisting of eight layers, see Fig. 3. The models employ cross-ply laminations characterized by stacking sequences with alternate plies oriented at 90° and 0° angles. The specific arrangement is pivotal in defining the mechanical behavior and response of the laminate, aspects that are the primary focus of the current investigation.

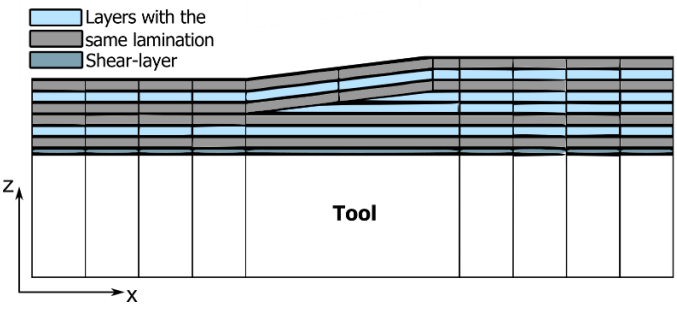

FIGURE 2: DROP-OFF LAYERS MODEL AND ITS REFERENCE SYSTEM.

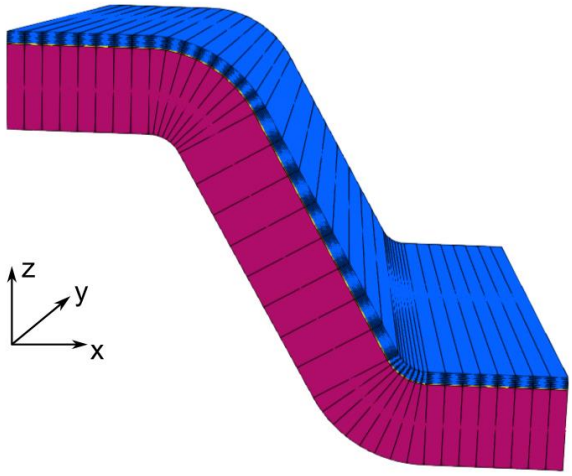

FIGURE 3: OMEGA-SHAPE MODEL AND ITS REFERENCE SYSTEM.

3.1 Drop-off layers model

The drop-off layers model is characterized by a multilayered composite material where each ply has a thickness of 0.2 mm. The laminate is positioned on a tool with a thickness of 8 mm, and an intermediate shear layer with a thickness of 0.12 mm is placed between the laminate and the tool.

Figure 2 shows the asymmetry in the laminate's thickness within the model: 1.6 mm on the right side, diminishing to 1.2 mm on the left. This gradation indicates a decrease in layers, leading to a varied overall thickness. The model measures 24 mm in the x-direction and 100 mm in the y-direction.

3.2 Omega-shape model

Figure 3 shows the geometry and the reference system of the Omega-shape model. The model is constructed from a multilayer composite material featuring a total thickness of 1.6 mm. This configuration includes a laminate positioned atop a 12 mm thick tooling base, with an intermediate shear layer, exactly one-tenth the thickness of the laminate, interposed between them. Geometrically, the model consists of two segments parallel to the x-axis, each measuring 20 mm long, and a flat segment inclined at a 60° angle to the z-axis. The first curved segment of the lamina features an internal radius of 17.16 mm and an external radius of 18.75 mm. In contrast, the second curved segment has an inner radius of 5.00 mm and an outer radius of 6.76 mm. Ultimate, the entire model spans 100 mm along the y-axis. Owing to symmetry concerning the plane x=0, only the model's right half is required for study.

4. NUMERICAL RESULTS AND DISCUSSION

The numerical results section is divided into two distinct subsections, each dedicated to one of the studied models. The primary objective is to investigate the residual deformations and stresses in the cured parts and analyze how the specific geometries and stacking sequences influence their final shapes. The analyses have been conducted over 48 steps, as this number offers a suitable balance between computational time and the accuracy of the results for all the study cases.

4.1 Drop-off layers results

This section focuses on the drop-off layer model. In the numerical model, L9 elements are utilized within the x-z plane of the cross-section, complemented by 10 B4 elements aligned along the model's longitudinal y-axis. The reference system of the three-dimensional model is given in Fig. 4. Two cross-ply stacking sequences, detailed in Table 1, are considered for the analysis.

ID LAM	STACKING SEQUENCE	
	6 LAYERS	8 LAYERS
1	90/0/90/90/0/90	90/0/90/0/0/90/0/90
2	0/90/0/0/90/0	0/90/0/90/90/0/90/0

TABLE 1: CROSS-PLY SIMMETRICAL STACKING SEQUENCES FOR THE EIGHT- AND SIX-LAYER LAMINATES.

In these models, 0° means the fibers are aligned parallel to the y-axis. The eight-layer configuration has a balanced laminate

structure. In contrast, the six-layer configuration is unbalanced. Within this setup, for LAM 1, the majority of plies are 90°, while in LAM 2, the majority are 0°.

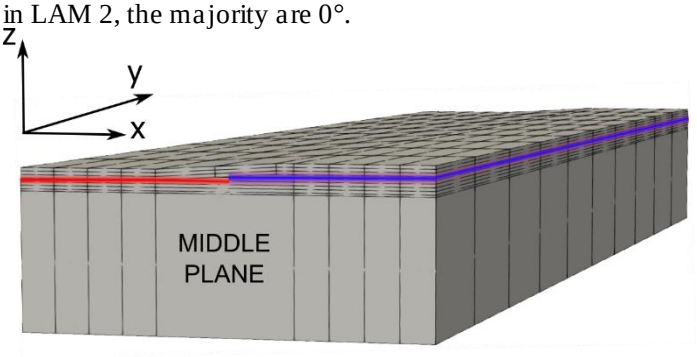

FIGURE 4 *REFERENCE SYSTEM OF THE DROP-OFF LAYER MODEL WITH THE MIDDLE PLANE MISMATCH.*

The drop-off model consists of two distinct laminates: one with eight (right) and another with six (left) layers. The analysis of each laminate is helpful to comprehend the deformation contributions from these two components. The plane at y=0 is constrained, ensuring zero displacements along the y-axis. The bottom plane is supported, and a symmetry condition is applied along the plane at x=0.

	8 LAYERS		6 LAYERS	
	LAM1	LAM 2	LAM 1	LAM 2
Max u_y [mm]	-0.076	-0.049	-0.120	-0.075

TABLE 2: *MAXIMUM DISPLACEMENTS ALONG THE Y DIRECTION FOR THE LAMINATE WITH 8 AND 6 LAYERS, LAM 1 AND LAM 2.*

Table 2 presents the maximum displacement in the y-direction at the free edge (y = 100 mm) in all cases studied. In both cases, the six-layer configuration exhibits more shrinkage in the y-direction compared to the eight-layer configuration. No out-of-the-plane bending is observed in these configurations. Many factors influence the ultimate shape of the drop-off layer model. For instance, the unbalanced structure of the six-layer side, the misalignment along the middle plane as shown in Fig. 4, and the differences in the y-direction displacement between six-layer and eight-layer configurations, see Table 2.

Figure 5 shows the displacement along the z-direction for the drop-off model.

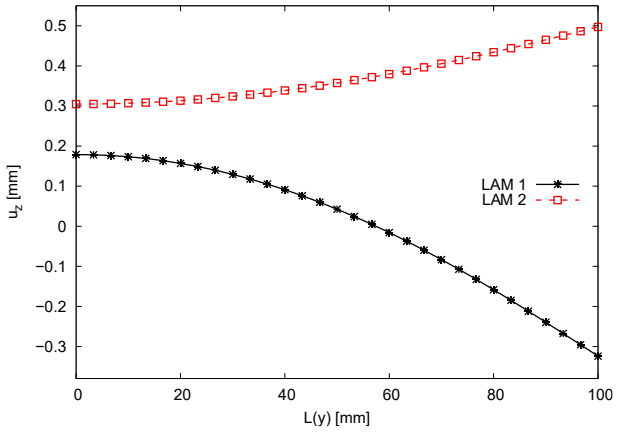

FIGURE 5 *TRANSVERSE DISPLACEMENT ALONG THE Y-DIRECTION OF THE MODEL FOR LAM 1 AND LAM 2.*

The stacking sequence of the model significantly influences the curvature's final shape. Specifically, LAM 1 has a final shape that bends towards negative z, while LAM 2 induces a bending in the positive z-direction. As shown in Fig. 6, the 90° plies are in a tension state, while the 0° are in compression. LAM 1, see Fig. 6(a), has the right side of the model with more plies under tension, and the structure tends to bend towards negative z. In contrast, in LAM 2, see Fig. 6(b), the right side is mainly in a compression state, leading to a curvature of the model in the positive z-direction.

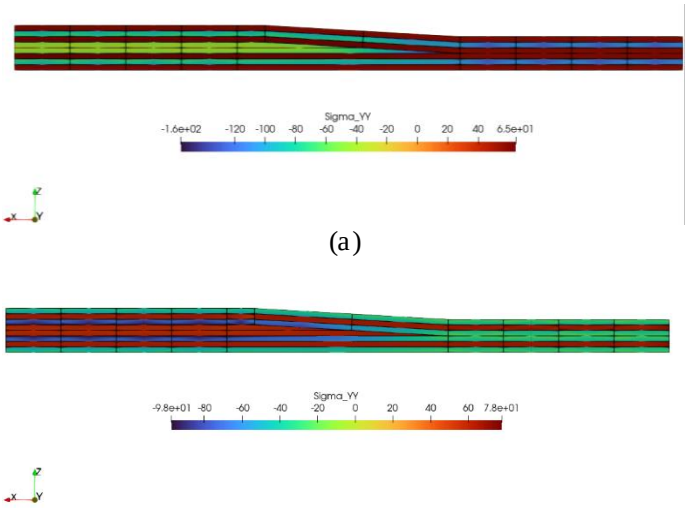

FIGURE 6 *RESIDUAL STRESS STATE σ_{yy} FOR (a) LAM 1 and (b) LAM 2.*

4.2 Omega-shape results

This section considers the Omega-shape case. In the numerical model, L9 elements are utilized within the x-z plane of the cross-section; see Fig. 3, and 1 B4 element is aligned along the model's longitudinal y-axis. Two cross-ply stacking sequences, see Table 3, are considered for the analysis.

ID LAM	STACKING SEQUENCE
1	90/0/90/0/0/90/0/90
2	0/90/0/90/90/0/90/0

TABLE 3: CROSS-PLY SYMMETRICAL STACKING SEQUENCES FOR THE OMEGA-SHAPE COMPONENT.

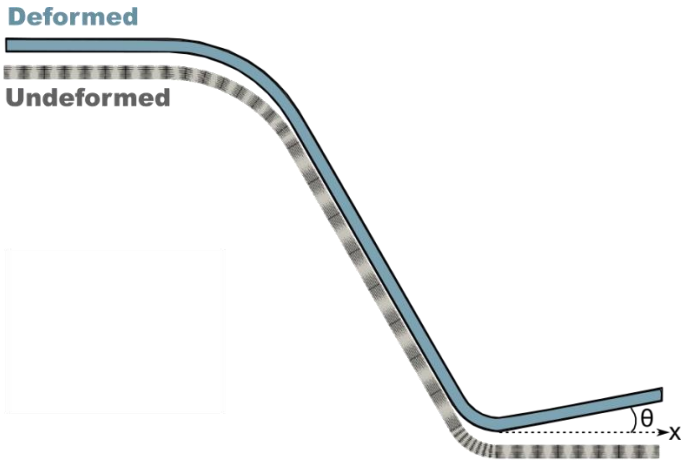

FIGURE 7 RESIDUAL DEFORMATION ANGLE BETWEEN THE UNDEFORMED AND THE DEFORMED STRUCTURE.

Two balanced and symmetrical configurations are considered, as outlined in Table 3, to assess the deformation of the final component. As previously discussed, the demolding process is a crucial phase for such complex structures. This phase poses a risk of distorting the intended shape of the model, emphasizing the importance of a carefully selected stacking sequence to control residual deformations. A primary concern in avoiding undesired deformations is its potential adverse effect on the compatibility of components during assembly. Therefore, the analysis focuses on the residual rotation angle, θ, as shown in Fig. 7.

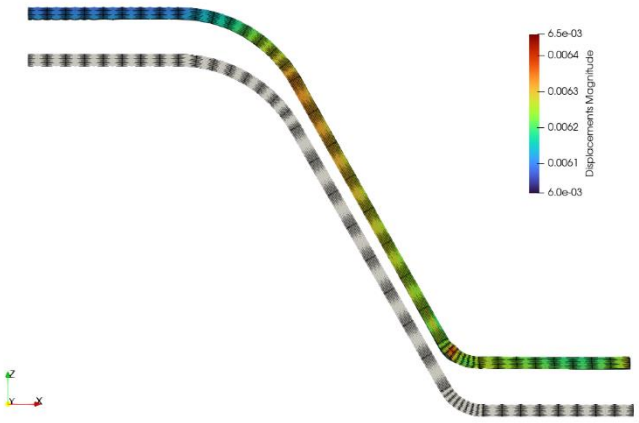

(a)

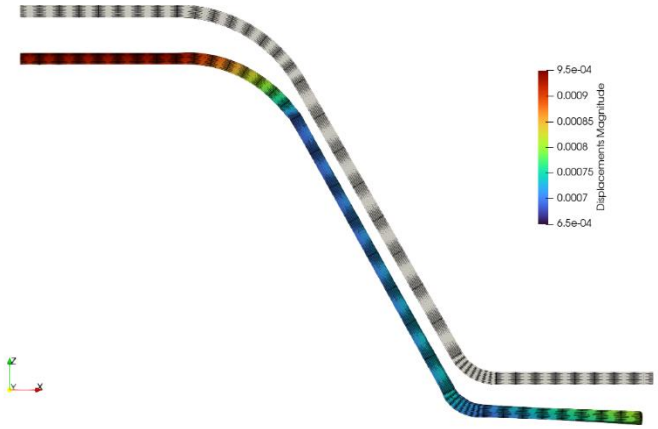

(b)

FIGURE 8 DISPLACEMENTS MAGNITUDE OF (a) LAM 1 (b) LAM 2, COMPARED TO THE UNDEFORMED CONDITION.

Figure 8 presents a visualization of the magnitude of the LAM 1 and LAM 2 displacements. Notably, the magnitude of displacements for LAM 1 is an order of magnitude greater than that for LAM 2. Moreover, the relative maximum rotation angles calculated at the middle plane of the model are listed in Table 4.

ID LAM	MAX ANGLE θ
1	6.42°
2	1.72°

TABLE 3 MAXIMUM ROTATION ANGLE θ FOR LAM 1 AND LAM 2.

Two omega-shape models under identical curing cycle load conditions, with slightly stacking sequences, significantly differ in the final deformation.

5. CONCLUSIONS

This paper proposes an efficient modeling approach for assessing deformations and residual stresses in composite parts undergoing curing in an autoclave. Based on refined one-dimensional kinematics models within the CUF framework, the numerical simulation predicts 3D displacements and stresses in complex configurations. The key findings of the study include:

- The laminate stacking sequence significantly affects the shape and bending behavior. In the drop-off model, LAM 1 bends towards negative z due to tension-dominated plies, while LAM 2 bends towards positive z due to compression-dominated plies.
- The stacking sequence of the laminate markedly influences the component's performance during the assembly phase. For LAM 1, the maximum angle reaches 6.42°, whereas for LAM 2, 1.72°.

ACKNOWLEDGEMENTS

This work was partly supported by the Italian Ministry of Foreign Affairs and International Cooperation (grant number US23GR12).

REFERENCES

[1] Residual Stress in Engineering Materials: A Review. A. Tabatabaeian, A. R. Ghasemi, M. M. Shokrieh, B. Marzbanrad, M. Baraheni and M. Fotouhi. Advanced Engineering Materials, 2021.

[2] An experimental and numerical study of curing deformation considering tool-part interaction for two-step curing tooling composite materials. Y. Xiao, D. Li, Z. Qian and Y. Li. Journal of Manufacturing Processes, 2023.

[3] The effect of ply drop-off on tensile strength of thermoplastic carbon fiber composite: a numerical and experimental study. D. Kane, G. Gomes, V. Macanhan and A. Ancelotti Jr. Engineering Computations, 2022.

[4] Analysis of process-induced deformations and residual stresses in curved composite parts considering transverse shear stress and thickness stretching. E. Zappino, N. Zobeiry, M. Petrolo, R. Vaziri, E. Carrera and A. Poursartip. Composite Structures journal, 2020.

[5] Experimental Investigation and Numerical Simulation of C-Shape Thin-Walled Steel Profile Joints. G. Taranu and I. O. Toma. Buildings, 2021.

[6] Quantitative validation of the analytical mode shapes of a beam-like structure with a Z-shaped configuration. W. Hu, F. Wang, D. Cao, J. Chen and J. Feng. Journal of Mechanical Science and Technology, 2019.

[7] Finite Element Analysis of Structures through Unified Formulation. E. Carrera, M. Cinefra, M. Petrolo, and E. Zappino. John Wiley and Sons, Ltd, Hoboken, New Jersey, USA, 2014.

[8] An Integrated Model of the development of Process-Induced Deformation in Autoclave Processing of Composite Structures, A. A. Johnston, The University of British Columbia, 1997.

[9] Hexcel, HexPly 8552 product data sheet, 2016.

[10] Hexcel, HexTow AS4 product data sheet.